

Structural Alterations in Scaffold Architecture in Response to Mechanical Stimuli

Blackstone BN^{1,2}, Wolever JD³ and Powell HM^{1,2,3*}

¹Department of Biomedical Engineering, The Ohio State University, Columbus, USA

²NSEC Center for Affordable Polymeric Biomedical Devices, The Ohio State University, Columbus, USA

³Department of Materials Science and Engineering, The Ohio State University, Columbus, USA

Abstract

Background: Though mechanical stimulation has been shown to improve mechanical properties of many engineered tissues, little is known about the impact of stimulation on scaffold architecture. In engineered tissues where the scaffold comprises a large portion of the tissue, mechanical signals are transferred from the external environment through the scaffold to the cells. Thus, a greater understanding of the architectural changes a scaffold experiences during mechanical stimulation may provide new knowledge on the communication between the cells and scaffold, during dynamic *in vitro* tissue development.

Methods: Two distinct scaffold architectures were fabricated via lyophilization or electro-spinning of collagen. Pore size of lyophilized scaffolds, fiber diameter and inter-fiber distance of electrospun scaffolds, and ultimate tensile strength, linear stiffness and stress relaxation rates for all scaffolds were determined, prior to mechanical stimulation. Scaffolds were then subjected to 0, 5, 10 or 20% static or cyclic strain. Alignment of lyophilized scaffold pores and electrospun fibers was then quantified after 4 and 7 days of mechanical stimulation.

Results: Lyophilized scaffolds displayed significant increases in pore area with magnitude of strain and duration of stimulation, and a pronounced alignment in pore orientation with the direction of strain. In contrast, electrospun samples showed only modest changes in architecture, in response to applied mechanical strain with small (1-5%) increased in fiber alignment compared to control, and no observed change in fiber morphology.

Conclusion: The current study showed the initial degree of interconnectivity between scaffold elements greatly impacted the scaffold response to mechanical stimulation. Non-woven electro-spun scaffold undergo very little micro structural reorganization during mechanical stimulation, while lyophilized collagen scaffolds undergo significant micro-structural changes. These differences in scaffold response suggest that large strain magnitudes may be required to excite cells within electro spun scaffolds, while modest strain magnitudes may result in significant changes in cellular behavior within lyophilized collagen sponges.

Introduction

Tissue engineering aims to generate organs and tissues *in vitro* that can replace diseased or non-functioning tissues, including skin, blood vessels, bone, cartilage and tendon [1-4]. Unfortunately, many engineered tissues are mechanically inferior to their native counterparts, and such mechanical mismatches lead to poor functioning or failure within the body. For example, engineered skin with reported ultimate tensile strengths between 0.01 and 0.7 MPa [5-8], is significantly weaker than native human skin (UTS=2.7-10 MPa [9]), causing it to be highly susceptible to mechanical damage in the early stages of engraftment [7-10]. Complications with mechanical mismatch have also been observed in tissue engineered blood vessels, many of which exhibit excellent cellular organization and patency when implanted [11,12], but require significant increases in strength to withstand the higher pressure of arterial circulation [13,14]. Thus, new strategies to improve the mechanical properties of engineered tissues are needed.

Mechanical forces are key regulators of tissue homeostasis and are essential for tissue formation, remodeling and normal function [9-15]. As a result, mechanical stimulation has frequently been employed to improve the organization and mechanics of engineered tissues [16-21]. For example, mechanical stimulation of mesenchymal stem cells within a porous collagen sponge led to significant increases in linear stiffness compared to controls [17]. Culturing keratinocytes and fibroblasts under static strain, within non-woven fibrous collagen scaffolds led to increases in skin tissue strength and stiffness, compared to non-strained controls [7]. While mechanical stimulation has been shown to be beneficial to *in vitro* tissue formation in many instances, the role of

stress/strain amplitude, frequency, duration of stimulation or scaffold architecture in this process is not well understood.

During mechanical stimulation, forces are exerted on the macroscopic engineered tissue containing cells, within a scaffold. In tissues where the scaffold comprises a large portion of the tissue, these mechanical signals are transferred from the external environment through the scaffold to the cells. As mechano-signal transduction involves internalization of external forces via the scaffold, scaffold properties such as pliability and stiffness are key factors in controlling the magnitude and type of cellular response to these signals. For example, extremely stiff scaffolds have been shown to reduce mechano-signal transduction, resulting in no significant change in gene expression when compared to unstimulated controls [22]. In order to utilize mechanical stimulation to its fullest potential, a greater understanding of the role scaffold properties in mechano-signal transduction is needed.

***Corresponding author:** Heather M. Powell, Department of Materials Science and Engineering, The Ohio State University, 243C Fontana Labs, Columbus, OH 43210, USA, Tel: 614-247-8673; Fax: 614-292-1537; E-mail: powell.299@osu.edu

Received October 07, 2012; **Accepted** November 20, 2012; **Published** November 22, 2012

Citation: Blackstone BN, Wolever JD, Powell HM (2012) Structural Alterations in Scaffold Architecture in Response to Mechanical Stimuli. J Tissue Sci Eng 3:122. doi:10.4172/2157-7552.1000122

Copyright: © 2012 Blackstone BN, et al. This is an open-access article distributed under the terms of the Creative Commons Attribution License, which permits unrestricted use, distribution, and reproduction in any medium, provided the original author and source are credited.

The goal of this study was to investigate structural changes in tissue engineering scaffolds during *in vitro* mechanical stimulation. To test the hypothesis that the nonwoven nature of electrospun scaffolds would result in significant fiber alignment and fiber thinning, after exposure to modest levels of static and cyclic strain (5-10%), collagen sponges with continuous connectivity between pores and non-woven collagen meshes, which contain no point contacts were exposed to static strain or cyclic strain, at increasing strain levels (5, 10, 20% strain). Changes in scaffold pore size, fiber diameter and overall morphology were assessed using confocal microscopy and quantified via image analysis.

Materials and Methods

Scaffold fabrication

To prepare reticulated collagen sponges, a 0.6 wt% solution of fibrous collagen from comminuted bovine hide (Kensley Nash, Exton, PA) in 0.5 M acetic acid was stirred on a magnetic stir plate for 48 hours at 4°C. The collagen-acetic acid solution was then homogenized using an IKA EUROSTAR 6000 homogenizer, at 4°C and 5400 rpm for six hours. After homogenization, the slurry was centrifuged at 1800 rpm for 10 min to remove all air bubbles, poured into Teflon-coated 316 L stainless steel casting frames (27 cm×18 cm×1mm), and frozen at -20°C for one hour. Prior to casting, collagen slurries were loaded with 0.01 wt/vol% Rhodamine B (Sigma-Aldrich, St. Louis, MO), to facilitate fluorescence imaging. The frozen collagen-acetic acid sheet was lyophilized and dehydrothermally cross-linked at 140°C for 24 hours. The scaffolds were disinfected in 70% ethanol for 24 hrs and rinsed thoroughly [23].

Non-woven, fibrous collagen scaffolds were electrospun using a 10% wt/vol. solution of acid-soluble collagen (Kensley Nash) in 1,1,1,3,3,3-Hexafluoro-2-propanol (HFP; Sigma-Aldrich). These solutions were loaded with 0.01 wt/vol% Rhodamine B and matrices were spun at a potential of 30 Kv onto an 8.5 cm² grounding plate at a distance of 20 cm. The electrospun scaffolds were physically cross-linked by vacuum dehydration at 140°C for 24 hrs, then chemically cross-linked in a solution of 5 mM EDC in 100% ethanol for 24 hrs [23]. The scaffolds were then disinfected in 70% ethanol for 24 hrs and rinsed thoroughly [23].

Scaffold morphology: Following DHT treatment, 6 mm punches of both the collagen sponge and collagen mesh were sputter coated with gold and examined using Scanning Electron Microscopy (SEM, FEI Sirion). SEM images were analyzed using Image J software to determine average pore size of the as-prepared sponge, fiber diameter of the mesh and inter-fiber distance of the mesh. All values were reported as average ± standard deviation.

Tensile testing: Mechanical properties of the as-fabricated scaffolds were measured by performing tensile tests on the samples (n=5 for each condition). Dog bone shaped specimens, with a gauge length of 20 mm and width of 4 mm, and a tab region of 10 mm×15 mm, were cut from each sample. Samples were loaded, hydrated into the grips of the tensile testing machine (Test Resources 100R; Shakopee, MN), with a layer of gauze between the grips and the sample, to prevent inadvertent tearing. Each sample was strained to failure at a rate of 2 mm/second. Linear stiffness and ultimate tensile strength was calculated from each sample, and reported as average ± standard deviation. Representative plots of stress vs. strain for each scaffold type were also reported. Relaxation tests were performed by straining the dog bone samples to 5, 10 or 20% at a rate of 2 mm/sec, and allowing holding at these maximum strains for 45 minutes, as load was continuously recorded. The raw force-time relaxation data were fit to

$$F(t) = At^{-n} \quad (1)$$

Where A is the force at t=0 and n is the time exponent. Equation 1 captures experimental trends from previous skin studies [24]. Average relaxation rate, n, ± standard deviation were reported.

Mechanical stimulation

Static strain: To evaluate the changes in scaffold morphology as a result of static mechanical strain, scaffolds (n=6 per condition) were cut into 2 cm×5 cm strips, loaded into strain devices, and strained to 0%, 5%, 10%, or 20% strain. Scaffolds were incubated in HBS and removed for analysis at day 4 or day 7. All scaffolds were hard mounted while still in strain devices to preserve their morphology. Microscope slides were inserted beneath the scaffolds while CC/Mount (Sigma-Aldrich) was applied to the scaffolds and allowed to harden. Scaffolds were then cut from the strain devices and analyzed using confocal microscopy (Olympus Fluoview 1000 Laser Scanning Confocal). Samples were examined with the principal axis of strain oriented vertically within the field of view, with electrospun scaffolds viewed with a 60X objective and sponges viewed with a 20X objective. Images were collected and fiber and pore orientation, with respect to the principal direction of stress was calculated from at least 300 fibers and 50 pores, respectively, from each group quantitatively via Image J software (<http://rsbweb.nih.gov/ij/>). For collagen sponges, changes in pore diameter and radius ratio were calculated from at least 50 pores per samples, and plotted as average value ± standard deviation. Fiber and pore orientation was binned (15° per bin), and plotted as frequency (% of total pores) per bin.

Cyclic strain: As cyclic strain is commonly used to stimulate engineered tissues, scaffolds were cut into strips (5 mm×30 mm), and placed into the grips of a uniaxial tensile tester with a heated biobath. Scaffolds were cyclically stimulated with amplitude of 5, 10 or 20%, at a frequency of 0.1 Hz. Following cyclic mechanical stimulation for 4 or 7 days, scaffolds were hard mounted, removed from the strain devices and processed for confocal microscopy, as above. Confocal images were analyzed using Image J software to determine fiber and pore orientation and average pore diameter, as above. The reported cyclic figures also include the static 0% strain condition for the corresponding day for reference.

Statistical analysis

Statistical analyses were performed using GraphPad (GraphPad Software, La Jolla, CA). One way ANOVA with Tukey post hoc tests were used, with p<0.05, considered statistically significant.

Results

As-fabricated scaffold morphology

Collagen scaffolds formed by lyophilization or electrospinning possessed dramatically different scaffold architectures. Collagen sponge (lyophilized collagen) contained thick reticulations of collagen (>7-10 μm) surrounding pores that were 138.61 ± 46.7 μm in diameter. All of the collagen reticulations were connected to one another in a highly open network of collagen (Figure 1A). In contrast, electrospun collagen scaffolds were comprised of thin, non-woven fibers which were closely packed (Figure 1B). With relatively short inter-fiber distances (6.83 ± 3.01 μm), the electrospun mat was significantly less porous than the lyophilized collagen sponge (Table 1).

As-fabricated scaffold mechanics

Lyophilized collagen scaffolds exhibited significantly higher

Ultimate Tensile Strength (UTS) and linear stiffness, and lower total elongation compared to electrospun collagen scaffolds (Table 1). At each strain level, the stress generated within the electrospun scaffolds was significantly lower than in the collagen sponges (Figure 2). Relaxation tests of the two scaffold types showed electrospun scaffolds exhibited

lower relaxation rates than the lyophilized scaffolds, when strained to 10 and 20% (Figure 3). The average relaxation rates (n from eqn. 1) for electrospun scaffolds were 0.158 ± 0.025 for 5% strain, 0.111 ± 0.01 for 10% strain, and 0.050 ± 0.003 for 20% strain. The average relaxation times for the lyophilized scaffolds were 0.139 ± 0.015 for 5% strain, 0.199 ± 0.007 for 10% strain, and 0.078 ± 0.001 for 20% strain.

Static strain scaffold morphology

Collagen scaffolds produced through both electro-spinning and lyophilization were held at fixed static strains of 0 (i.e. no strain), 5, 10, and 20% for four and seven days, and examined using confocal microscopy to assess structural changes (Figure 4 and 5). After hydration and 4 days incubation, pores of lyophilized scaffolds were rounded, approximately equiaxed, and contained a distribution of pore sizes (Figure 4). After application of a static, constant strain, pore shape began to change, with an increase in observed pore size and shift toward an elliptical morphology, with the long axis oriented with

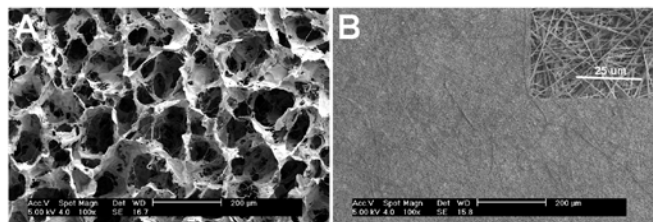


Figure 1: Scanning electron micrographs of the lyophilized collagen scaffold (A) and the electrospun collagen scaffold (B).

Scaffold Type	Fiber Diameter (μm)	Pore Diameter/ Inter-fiber Distance (μm)	Porosity	Maximum Load (mN)	Linear Stiffness (mN/mm)	% Elongation
Electrospun Mat	0.69 ± 0.38	6.83 ± 3.01	76.1 ± 3.6	148.3 ± 11.8	8.0 ± 0.05	154.2 ± 9.3
Lyophilized Sponge	-	138.61 ± 46.7	89.2 ± 3.6	189.0 ± 37.2	26.4 ± 6.8	73.6 ± 8.4

Table 1: Structural and mechanical properties of collagen scaffold fabricated via electro spinning or lyophilisation.

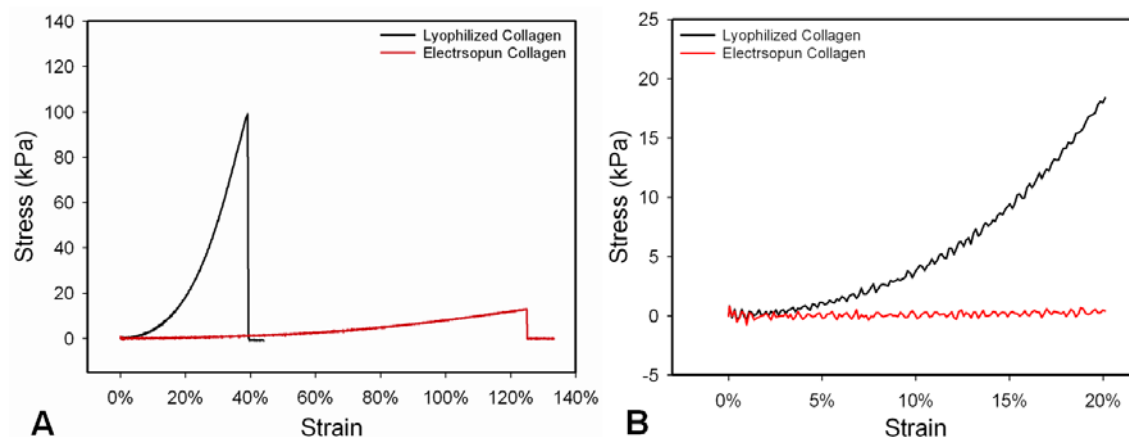


Figure 2: Representative stress vs. strain plots of lyophilized and electrospun collagen tensile tests (A) with a focus on the initial response (B).

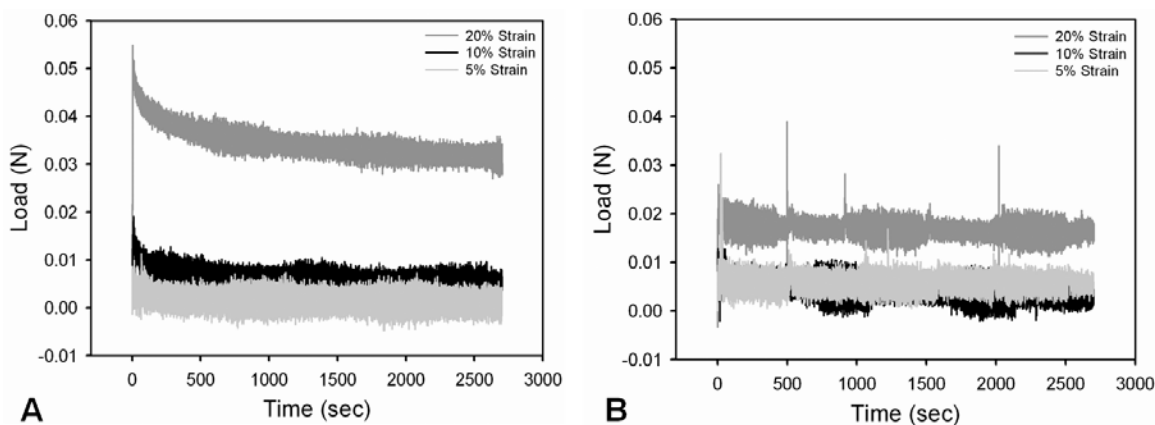
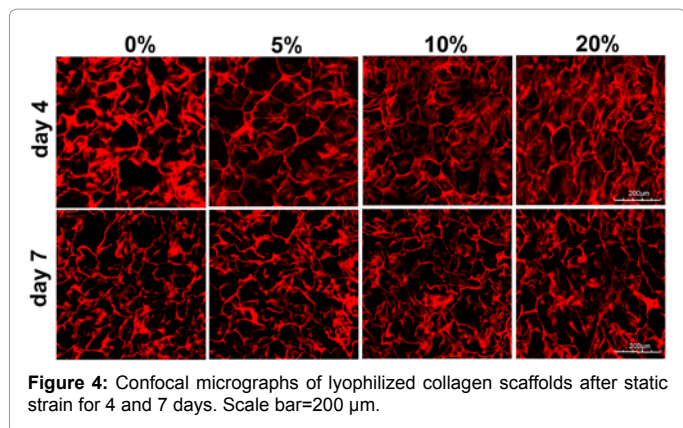
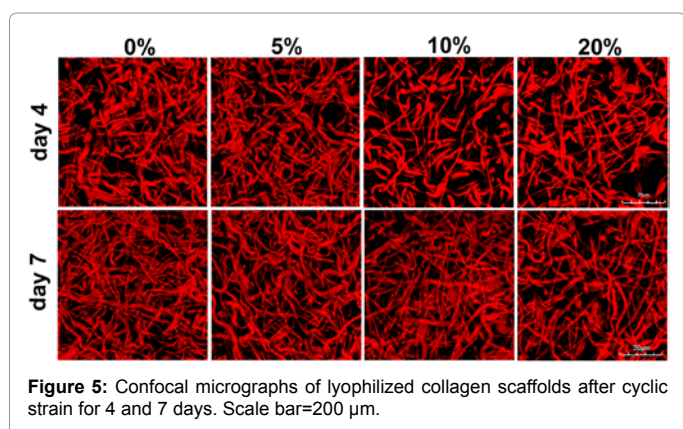


Figure 3: Relaxation curves for collagen scaffolds formed by A) lyophilization and B) electrospinning strained to 5%, 10% or 20% strain and held for 45 minutes.



the principal direction of strain. With increased strain, pores became more elliptical and aligned (Figure 4, upper). In contrast, this trend of elongated pore shapes did not remain after 7 days in culture, when the strain magnitude was less than 20% (Figure 4, lower). At day 7, pore reticulations were more tortuous and irregularly shaped.

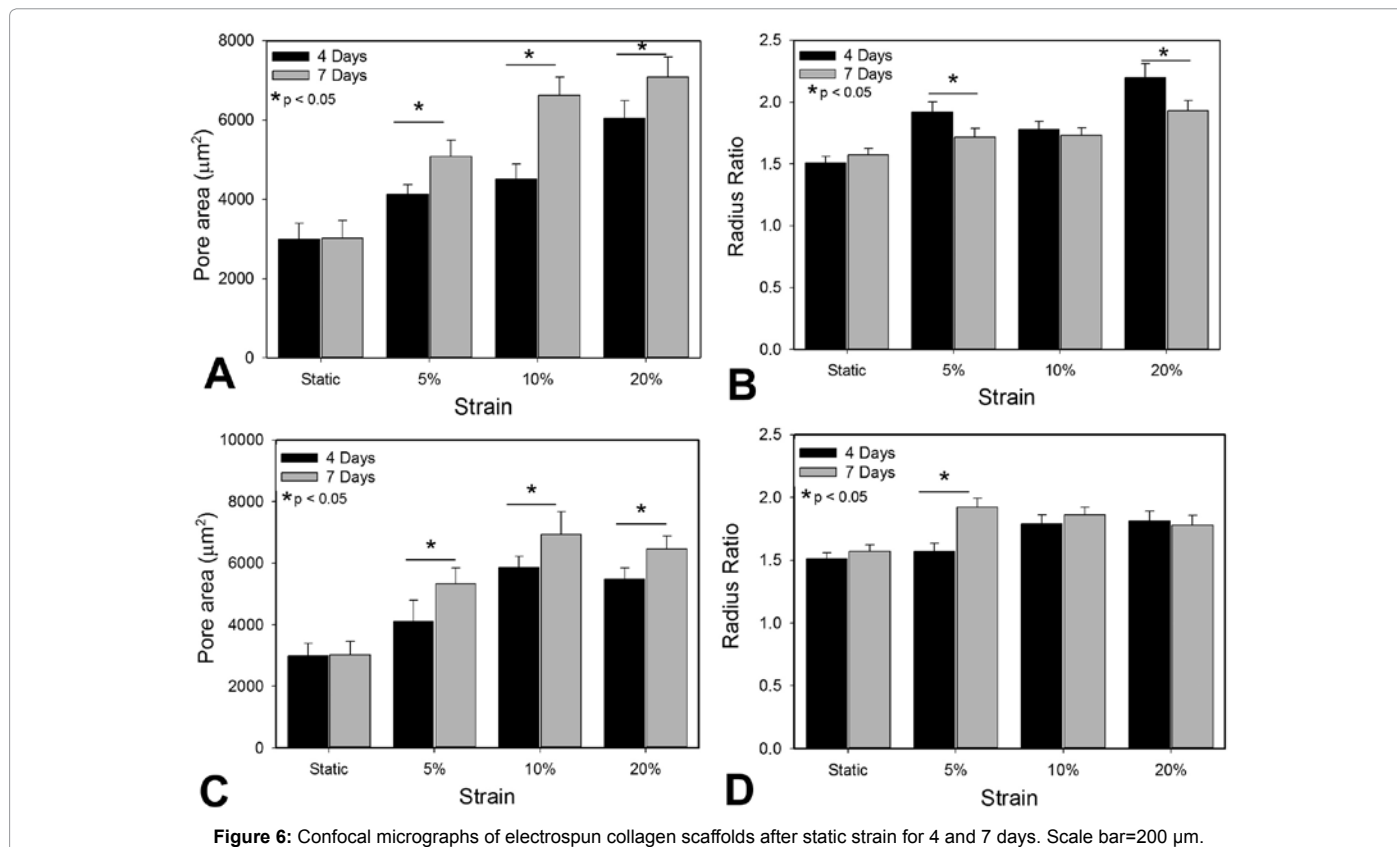
Hydrated electrospun scaffolds were comprised of dense, randomly oriented, tortuous fibers, approximately 4 μ m in diameter (Figure 5). As the magnitude of applied strain increased, the fibers appeared to straighten and become less tortuous (Figure 5, upper). However, no significant change in fiber orientation was observed. As the duration of strain application increased, fiber orientation appeared to increase slightly in the 10% and 20% (Figure 5).



Quantitative analysis of the confocal images confirmed that pore area of lyophilized scaffolds significantly increased with magnitude of strain and time (with the exception of the 0% static condition), while the radius ratio did not significantly change (Figure 6A and 6B). Lyophilized scaffolds showed increased pore alignment with increased strain magnitude and time, with the majority of pores oriented within $\pm 15^\circ$ of the direction of applied strain (0°) (Figure 7A and 7B). For electrospun scaffolds, the percentage of fiber within $\pm 15^\circ$ of the principal direction of strain, increased by only 5% from the no strain condition to 20% strain (Figure 8 A and 8B).

Cyclic strain scaffold morphology

Following cyclic strain, pores in became elongated and oriented in the direction of strain (Figure 9, upper). Pore size distribution appeared to shift towards fewer very large pores with numerous smaller pores, as the magnitude of strain increased. After 7 days of cyclic strain, pore diameter increased, and pore wall shape became more irregular than



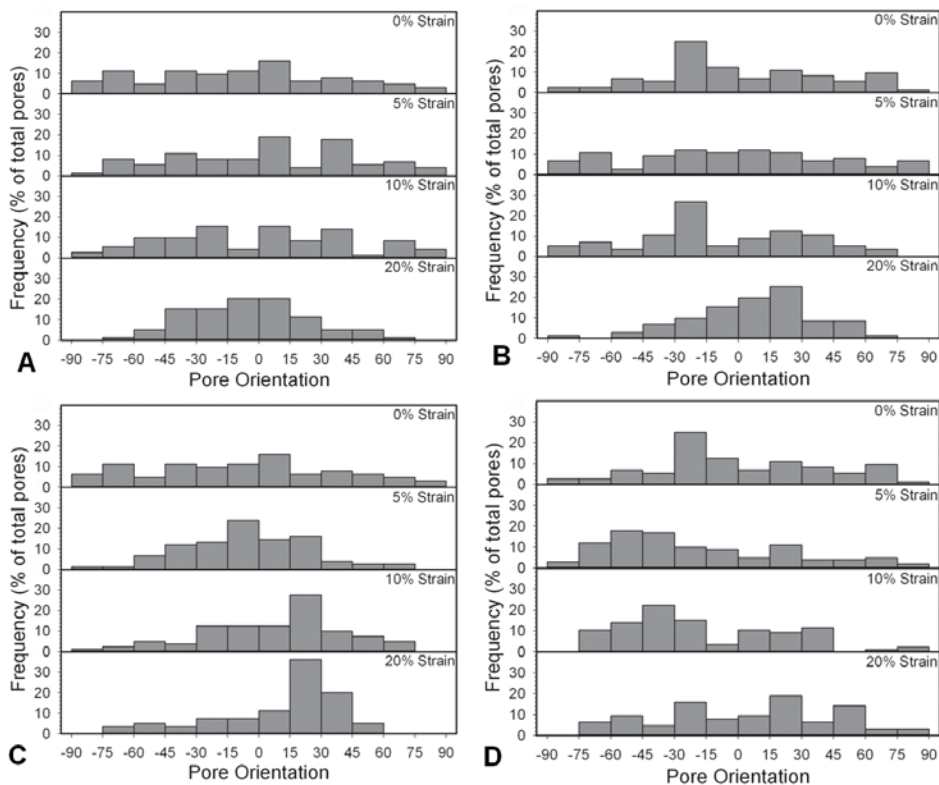


Figure 7: Confocal micrographs of electrospun collagen scaffolds after cyclic strain for 4 and 7 days. Scale bar=200 μ m.

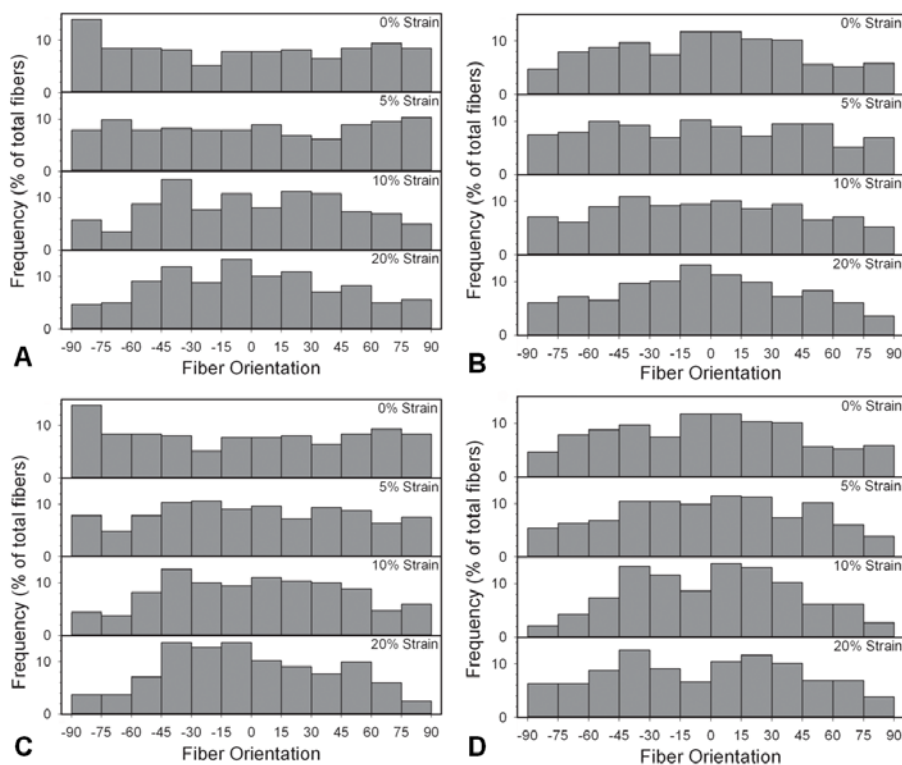


Figure 8: Pore morphology after exposure to strain for 4 and 7 days. A&C) Pore area and B&D) pore radius ratio as a function of A&B) static strain or C&D) cyclic strain. Pore area significantly increases with strain magnitude after 4 days ($p < 0.05$) and after 7 days ($p < 0.01$) of static strain. Pore area increases in response to cyclic strain up to 10% strain after 4 and 7 days of stimulation ($p < 0.05$).

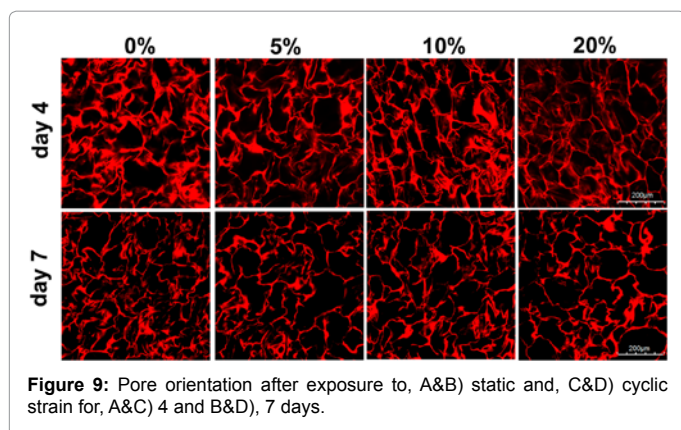


Figure 9: Pore orientation after exposure to, A&B) static and, C&D) cyclic strain for, A&C) 4 and B&D), 7 days.

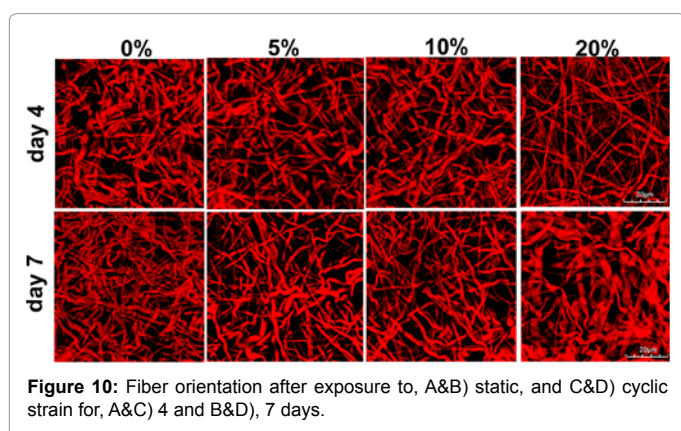


Figure 10: Fiber orientation after exposure to, A&B) static, and C&D) cyclic strain for, A&C) 4 and B&D), 7 days.

the 4 day counterparts, with a greater distribution of pore sizes present in each image (Figure 9, lower). Image analysis revealed that under cyclic strain, pore area of lyophilized scaffolds again increased with strain magnitude and time, with the exception of 20% applied strain. At 20% strain, pore area was slightly decreased from 10% strain at both days 4 and 7 (Figure 6C and 6D). On day 4, the long axes of pores in lyophilized scaffolds became more aligned in the direction of applied strain (Figure 7C). The most extreme increase in alignment was seen in scaffolds subjected to 20% strain, with greater than 45% of all pores oriented between 0 and 30 degrees from the direction of strain (Figure 7C). At day 7, pore orientation was more randomly distributed, with no significant change in alignment compared to control (Figure 9D).

Fibers under cyclic strain were less tortuous with increasing amplitude of cyclic strain, after 4 days of exposure (Figure 10, upper). After 7 days of exposure, the observed fiber straightening with strain amplitude was less prominent (Figure 10, lower). Electro-spun scaffolds showed very modest changes in fiber orientation, in response to applied strain. At 4 days, the maximum fiber alignment was seen in scaffolds strained to 20%, however the total percent of fibers $\pm 15^\circ$ from the principle direction of strain was less than 25% of the total fibers analyzed (Figure 8C). Continued high cyclic strain resulted in bimodal distributions of fiber alignment, with small concentrations of fibers aligned 30° to the left and right of applied strain (Figure 8D).

Discussion

As the fibers in the electrospun collagen scaffolds were not bonded together (Figure 1B), it was expected that the fiber architecture would change more easily in response to external uniaxial strain,

and electrospun fibers would reorient themselves, along the principle direction of stress. Current results indicate that the electrospun collagen scaffolds experience little microstructural reorganization, after exposure to both static and cyclic strain. This is in contrast to prior studies which indicated that the constant application of 10% or greater uniaxial strain for 7 days significantly increased electrospun collagen fiber orientation, with the vast majority of fibers aligned $\pm 15^\circ$ of the principal direction of strain [7]. One possible mechanism for this difference in observed outcome is the method of sample preparation. In the prior study, scaffolds were dehydrated, while in the testing rigs for scanning electron microscopy. As the electro-spun collagen fibers are dehydrated, they shrink both radially (as evidenced by the significant difference in fiber diameter between hydrated and dry fibers; figure 1 and 5) and laterally. This could cause a significant increase in fiber alignment as the fibers dry and contract. In contrast, the current study mounts the electrospun scaffolds in their hydrated state, and while they are still in the mechanical stimulation rigs. As hard mount medium is used the structure of the scaffolds is "locked-in", without significant dehydration.

Electro-spun collagen scaffolds in their hydrated state are also extremely compliant, and are comprised of wavy, Tortuous (T) fibers [25]. During uniaxial tensile testing, the stress-strain curve contained a significant toe-in region, and strains well above 20% elongation (Figure 2) were required to generate appreciable stress. Within this toe-in region, fiber straightening and re-orientation occurs until fibers become straight and aligned, and thus experience significant loading. In prior studies, it has been observed that electrospun collagen fibers can have a tortuosity (total length of fiber divided by the length of a straight line connecting each end of the fiber), as large as 1.6 with $\sim 10\%$ of collagen fibers, having T-values > 1.4 , indicating that each fiber could be extended by $> 40\%$ before they are straightened [25]. It is likely that in the current electrospun scaffolds, applied strain straightens the fibers (i.e. reduces T), but does not reach a magnitude large enough to generate both fiber straightening and subsequent rotation and reorientation. Confocal images show that fibers under static strain begin to straighten at 10-20% strain, but do not have significant alignment (Figure 5). This phenomenon was also observed in collagen fibers within bovine pericardium, where 15% or greater uniaxial strain is needed to generate significant collagen fiber alignment [26].

In contrast to the electrospun collagen scaffolds, lyophilized collagen scaffolds underwent significant microstructural changes during mechanical stimulation. Under both static and cyclic stimulation, a general trend of increasing pore area was observed with strain magnitude and time of stimulation (Figure 6). Additionally, the long axis of the pores became aligned with the principal direction of strain, with significant alignment following 20% static strain for 4 and 7 days, and with 5% or greater cyclic strain for 4 days. As the lyophilization or freeze drying process forms continuous networks of collagen, the applied strain will be transferred throughout the scaffold more uniformly than in the electrospun scaffolds. The applied strain stretches the collagen reticulations, increasing the observed pore area (Figure 6). Interestingly, pore area in the 20% cyclic group decreased slightly and had no pore alignment. It is proposed that at these magnitudes of strain, micro-cracks are generated in the reticulations of the scaffold, which eventually break after continued fatigue, allowing the collagen to recoil in those areas and pores to recover their initial size.

Characterizing the response of scaffolds used for tissue engineering to different mechanical stimuli allows for better prediction of how

external forces will be transferred through the scaffold to the cells. Prior studies have shown that the local strain applied to the cell can often deviate significantly from the macroscopic strain applied to the construct. On a deformable membrane such as silicone, cell strain can be 30% less than the strain delivered to the membrane [27]. As different cell types can be more sensitive to mechanical stimuli [28-31], it is important to be able to predict the amount of force or strain applied to the cells, not simply the amount of force or strain applied to the scaffold+cell construct. Therefore, it is extremely important to consider scaffold architecture, when determining a mechanical stimulation profile for a specific cell type.

Conclusions

Mechanical stimulation of engineered tissue during *in vitro* development has widely been used to enhance mechanical properties. As mechanical signals are transferred from the external environment to the cells via the scaffold, it is important to understand the effect of stimulation on scaffold properties. The current study showed that electrospun scaffold undergo very little microstructural reorganization, in response to mechanical strains up to 20%, while lyophilized collagen scaffolds undergo significant microstructural changes, including pore enlargement and pore alignment at strains as low as 5%. These differences in scaffold response suggest that large strain magnitudes may be required to excite cells within electrospun scaffolds, while modest strain magnitudes may result in significant changes in cellular behavior within lyophilized collagen sponges.

Acknowledgements

This material is based, in part, upon work supported by the National Science Foundation under Grant No. EEC-0914790. The authors would like to thank the Campus Microscopy and Imaging Facility, and the Campus Electron Optics Facility, for use of the confocal microscope and scanning electron microscope, respectively.

References

1. Boyce ST, Kagan RJ, Yakuboff KP, Meyer NA, Rieman MT, et al. (2002) Cultured skin substitutes reduce donor skin harvesting for closure of excised, full-thickness burns. *Ann Surg* 235: 269-279.
2. Hutmacher DW (2000) Scaffolds in tissue engineering bone and cartilage. *Biomaterials* 21: 2529-2543.
3. Altman GH, Horan RL, Lu HH, Moreau J, Martin I, et al. (2002) Silk matrix for tissue engineered anterior cruciate ligaments. *Biomaterials* 23: 4131-4141.
4. L'Heureux N, Pâquet S, Labbé R, Germain L, Auger FA (1998) A completely biological tissue-engineered human blood vessel. *FASEB J* 12: 47-56.
5. Powell HM, Boyce ST (2006) EDC cross-linking improves skin substitute strength and stability. *Biomaterials* 27: 5821-5827.
6. Powell HM, Boyce ST (2009) Engineered human skin fabricated using electrospun collagen-PCL blends: morphogenesis and mechanical properties. *Tissue Eng Part A* 15: 2177-2187.
7. Powell HM, McFarland KL, Butler DL, Supp DM, Boyce ST (2010) Uniaxial strain regulates morphogenesis, gene expression, and tissue strength in engineered skin. *Tissue Eng Part A* 16: 1083-1092.
8. LaFrance H, Yahia L, Germain L, Guillot M, Auger FA (1995) Study of the tensile properties of living skin equivalents. *Biomed Mater Eng* 5: 195-208.
9. Silver FH, Freeman JW, DeVore D (2001) Viscoelastic properties of human skin and processed dermis. *Skin Res Technol* 7: 18-23.
10. Boyce ST, Supp AP, Wickett RR, Hoath SB, Warden GD (2000) Assessment with the dermal torque meter of skin pliability after treatment of burns with cultured skin substitutes. *J Burn Care Rehabil* 21: 55-63.
11. Niklason LE, Gao J, Abbott WM, Hirschi KK, Houser S, et al. (1999) Functional arteries grown in vitro. *Science* 284: 489-493.
12. Liu JY, Swartz DD, Peng HF, Gugino SF, Russell JA, et al. (2007) Functional tissue-engineered blood vessels from bone marrow progenitor cells. *Cardiovasc Res* 75: 618-628.
13. Yao L, Liu J, Andreadis ST (2008) Composite fibrin scaffolds increase mechanical strength and preserve contractility of tissue engineered blood vessels. *Pharm Res* 25: 1212-1221.
14. Swartz DD, Russell JA, Andreadis ST (2005) Engineering of fibrin-based functional and implantable small-diameter blood vessels. *Am J Physiol Heart Circ Physiol* 288: H1451-H1460.
15. Ladd MR, Lee SJ, Atala A, Yoo JJ (2009) Bioreactor maintained living skin matrix. *Tissue Eng Part A* 15: 861-868.
16. Stegemann JP, Nerem RM (2003) Phenotype modulation in vascular tissue engineering using biochemical and mechanical stimulation. *Ann Biomed Eng* 31: 391-402.
17. Nirmalanandhan VS, Juncosa-Melvin N, Shearn JT, Boivin GP, Galloway MT, et al. (2009) Combined effects of scaffold stiffening and mechanical preconditioning cycles on construct biomechanics, gene expression, and tendon repair biomechanics. *Tissue Eng Part A* 15: 2103-2111.
18. Datta N, Pham QP, Sharma U, Sikavitsas VI, Jansen JA, et al. (2006) In vitro generated extracellular matrix and fluid shear stress synergistically enhance 3D osteoblastic differentiation. *Proc Natl Acad Sci U S A* 103: 2488-2493.
19. De Croos JN, Dhaliwal SS, Grynopas MD, Pilliar RM, Kandel RA (2006) Cyclic compressive mechanical stimulation induces sequential catabolic and anabolic gene changes in chondrocytes resulting in increased extracellular matrix accumulation. *Matrix Biol* 25: 323-331.
20. Freyria AM, Yang Y, Chajra H, Rousseau CF, Ronzière MC, et al. (2005) Optimization of dynamic culture conditions: effects on biosynthetic activities of chondrocytes grown in collagen sponges. *Tissue Eng* 11: 674-684.
21. Isenberg BC, Williams C, Tranquillo RT (2006) Small-diameter artificial arteries engineered in vitro. *Circ Res* 98: 25-35.
22. Babalola OM, Bonassar LJ (2009) Parametric finite element analysis of physical stimuli resulting from mechanical stimulation of tissue engineered cartilage. *J Biomech Eng* 131: 061014.
23. Powell HM, Boyce ST (2008) Fiber density of electrospun gelatin scaffolds regulates morphogenesis of dermal-epidermal skin substitutes. *J Biomed Mater Res A* 84: 1078-1086.
24. Corr DT, Gallant-Behm CL, Shrive NG, Hart DA (2009) Biomechanical behavior of scar tissue and uninjured skin in a porcine model. *Wound Repair Regen* 17: 250-259.
25. Ebersole GC, Paranjape H, Anderson PM, Powell HM (2012) Influence of hydration on fiber geometry in electrospun scaffolds. *Acta Biomater* 8: 4342-4348.
26. Liao J, Yang L, Grashow J, Sacks MS (2005) Molecular orientation of collagen in intact planar connective tissues under biaxial stretch. *Acta Biomater* 1: 45-54.
27. Rosenblatt N, Hu S, Chen J, Wang N, Stamenovic D (2004) Distending stress of the cytoskeleton is a key determinant of cell rheological behavior. *Biochem Biophys Res Commun* 321: 617-622.
28. Awolesi MA, Sessa WC, Sumpio BE (1995) Cyclic strain upregulates nitric oxide synthase in cultured bovine aortic endothelial cells. *J Clin Invest* 96: 1449-1454.
29. Clark CB, McKnight NL, Frangos JA (2002) Strain and strain rate activation of G proteins in human endothelial cells. *Biochem Biophys Res Commun* 299: 258-262.
30. Owan I, Burr DB, Turner CH, Qiu J, Tu Y, et al. (1997) Mechanotransduction in bone: osteoblasts are more responsive to fluid forces than mechanical strain. *Am J Physiol* 273: C810-C815.
31. Neidlinger-Wilke C, Wilke HJ, Claes L (1994) Cyclic stretching of human osteoblasts affects proliferation and metabolism: a new experimental method and its application. *J Orthop Res* 12: 70-78.